

# A ROBUST SIMILARITY MEASURE FOR NONRIGID IMAGE REGISTRATION WITH OUTLIERS

Stefan Pszczolkowski, Stefanos Zafeiriou, Christian Ledig and Daniel Rueckert

Department of Computing, Imperial College London, London, UK.

## ABSTRACT

Nonrigid image registration is a widely used technique in medical imaging. While most methods work very well on images without pathologies or artefacts, there is a high need for improved robustness on images from pathological subjects and acquisitions with artefacts such as intensity inhomogeneity. In this paper, we propose a novel similarity measure based on normalised gradients for nonrigid registration, which is robust on images with intensity inhomogeneities or pathologies. We provide both theoretical and experimental proof of the robustness and evaluate the approach on manually segmented and simulated pathological images. Compared to normalised mutual information and to an alternative similarity also based on normalised gradients, we obtain significant overlap improvements for images with intensity inhomogeneities. We further confirm improved robustness on images with simulated tumours.

## 1. INTRODUCTION

Nonrigid image alignment is a crucial requirement in a variety of applications in medical imaging, including automatic segmentation, motion tracking and morphometric analysis. A large number of different successful approaches have been proposed to the problem of nonrigid image registration [1]. However, since most of the research focuses on registration of images with differences that can always be matched, there is a significant need for improved robustness on images with structures that appear just in one of the images, such as pathologies, and on images with acquisition artefacts like intensity inhomogeneity.

In medical imaging, several methods have been proposed for registration of images with mismatches, focusing on robustness [2], tumour models [3] or bayesian models [4]. However, all these methods need a prior knowledge of what a “mismatch” is in order to detect and/or ignore them. Additionally, a number of methods based on mutual information have been proposed to reduce the effect of intensity inhomogeneities in the registration [5, 6, 7].

The concept of normalised image gradients was introduced to the field of medical image registration by Pluim *et al.* [8]. In this work, normalised mutual information (NMI) [9] is weighted voxel-wise by the normalised image gradients in order to incorporate spatial information. After this initial work, the first similarity based solely on normalised gradients was proposed by Haber *et al.* [10]. Since its introduction, this measure has been successfully utilised [11, 12, 13]. However, as we show in this paper, this cost functional is less robust to image inhomogeneities and is affected when gross outliers, such as lesions or tumours, are present in the images.

To the best of our knowledge, there is no previously proposed similarity measure in nonrigid image registration that is robust to both imaging artefacts such as intensity inhomogeneities caused by bias fields and outliers in the images, e.g. in form of pathology.

To this end, we utilise a simple, but effective similarity measure based on the angle between gradient orientations, which are obtained from the normalised image gradients. A similar approach has been recently successfully applied for the robust affine alignment of facial images [14] and shown to be robust towards occlusions and changes in illumination. Specifically, we employ this similarity measure within a widely and successfully used nonrigid registration framework based on free-form deformations (FFD) [15]. We provide theoretical evidence of its robustness and evaluate on manually segmented data. We obtain favourable overlap measures for images with intensity inhomogeneities. We also confirm robustness of the proposed similarity measure on simulated pathological data from a tumour database.

## 2. METHOD

### 2.1. Proposed similarity measure

Image registration can be regarded as an energy minimisation problem. A typical energy functional  $E$  is composed of a data term  $E_D$  and a regularisation term  $E_R$ .  $E_D$  measures the degree of alignment of a target (fixed) image  $I_0$  and a source (moving) image  $I$ .  $E_R$  imposes smoothness on the deformation field that aligns the images. Hence,  $E = E_D + \lambda E_R$ , where the parameter  $\lambda \geq 0$  is the weight of the regularisation.

In [10], the authors use the observation that a target and a source image come into alignment when the square of the cosine of the angle between the target and warped source gradient orientations is maximised. In contrast, we propose to adopt the similarity measure introduced by Tzimiropoulos *et al.* [14], which corresponds to only the cosine (not squared) between gradient orientations, and introduce it into the problem of nonrigid medical image registration. Hence, we propose to utilise the following data energy functional

$$E_D(T) = - \sum_{k \in \Omega} \cos \phi(\nabla I_0(k), (T \circ \nabla I)(k)). \quad (1)$$

Here,  $\Omega$  is the set of indices corresponding to the target image support,  $\phi(\cdot, \cdot)$  is the angle between two gradient orientations,  $T$  is the current spatial transformation, and  $T \circ \nabla I$  denotes the warped source gradient, which is obtained by applying the spatial transformation  $T$  independently on the  $x$ ,  $y$  and  $z$  components of  $\nabla I$ . Our proposed data energy term in (1) can be expressed in terms of the dot product  $\langle \cdot, \cdot \rangle$  between gradients

$$E_D(T) = - \sum_{k \in \Omega} \frac{\langle \nabla I_0(k), (T \circ \nabla I)(k) \rangle}{\|\nabla I_0(k)\| \|(T \circ \nabla I)(k)\|} \quad (2)$$

### 2.2. Numerical stability

As discussed in [10], it is not possible to use normalised gradient fields directly due to discontinuities in the differentiation. We thus

compute the data energy term using regularised normalised gradient fields as presented in [13]

$$E_D(T) = - \sum_{k \in \Omega} \frac{\langle \nabla I_0(k), (T \circ \nabla I)(k) \rangle_{\varrho, \tau}}{\|\nabla I_0(k)\|_{\varrho} \|(T \circ \nabla I)(k)\|_{\tau}}, \quad (3)$$

where  $\langle \cdot, \cdot \rangle_{\varrho, \tau} = \langle \cdot, \cdot \rangle + \varrho \tau$  and  $\|\cdot\|_* = \sqrt{\langle \cdot, \cdot \rangle_{*,*}}$ . In this work,  $\varrho$  and  $\tau$  are not user-defined parameters as in [13]. Instead, they are computed following an automatic choice based on total variation

$$\varrho = \frac{\eta}{V_{I_0}} \sum_{k \in \Omega_{I_0}} |\nabla I_0(k)|, \quad \tau = \frac{\eta}{V_I} \sum_{k \in \Omega_I} |\nabla I(k)| \quad (4)$$

where  $\eta > 0$  is a parameter for noise filtering and  $V_*$  is the volume of interest in the image domain  $\Omega_*$ .

### 2.3. Robustness of the proposed similarity measure

#### 2.3.1. Robustness against intensity inhomogeneities

A significant advantage of normalised gradient-based methods is their invariance towards low frequency intensity changes, as we now demonstrate. Consider an image signal  $M$  with no intensity inhomogeneities and a multiplicative, non-negative bias field  $B$  which is assumed to be smooth, i.e., constant in the small neighborhood  $\mathcal{N}(k) = (\Delta k_x, \Delta k_y, \Delta k_z)$ . This means  $B(p) \approx B(k), \forall p \in \mathcal{N}(k)$ . We have for  $\Delta k_x$

$$\begin{aligned} I_{\text{BIAS}}(k) &= M(k)B(k) \\ I_{\text{BIAS}}(k + \Delta k_x) &= M(k + \Delta k_x)B(k + \Delta k_x), \end{aligned} \quad (5)$$

and given that  $B(k)$  is constant within the neighborhood

$$\begin{aligned} \frac{\partial I_{\text{BIAS}}(k)}{\partial x} &= \lim_{\Delta k_x \rightarrow 0} \frac{I_{\text{BIAS}}(k + \Delta k_x) - I_{\text{BIAS}}(k)}{\Delta k_x} \\ &\approx \lim_{\Delta k_x \rightarrow 0} \frac{B(k)(M(k + \Delta k_x) - M(k))}{\Delta k_x} \\ &= B(k) \frac{\partial M(k)}{\partial x}. \end{aligned} \quad (6)$$

Using this result, we now show that the proposed cost function is indeed robust to locally constant bias fields using the normalisation scheme in (3). If the contributions of  $\varrho$  and  $\tau$  are disregarded, we have

$$\frac{\frac{\partial I_{\text{BIAS}}(k)}{\partial x}}{\sqrt{\left(\frac{\partial I_{\text{BIAS}}(k)}{\partial x}\right)^2 + \left(\frac{\partial I_{\text{BIAS}}(k)}{\partial y}\right)^2 + \left(\frac{\partial I_{\text{BIAS}}(k)}{\partial z}\right)^2}}. \quad (7)$$

By using equation (6) we obtain

$$\frac{B(k) \frac{\partial M(k)}{\partial x}}{\sqrt{\left(B(k) \frac{\partial M(k)}{\partial x}\right)^2 + \left(B(k) \frac{\partial M(k)}{\partial y}\right)^2 + \left(B(k) \frac{\partial M(k)}{\partial z}\right)^2}}. \quad (8)$$

Here we observe that  $B(k)$  vanishes, yielding

$$\frac{\frac{\partial M(k)}{\partial x}}{\sqrt{\left(\frac{\partial M(k)}{\partial x}\right)^2 + \left(\frac{\partial M(k)}{\partial y}\right)^2 + \left(\frac{\partial M(k)}{\partial z}\right)^2}}. \quad (9)$$

Equations (5)-(9) are analogous for  $\Delta k_y$  and  $\Delta k_z$ . This leads to

$$\frac{\nabla I_{\text{BIAS}}(k)}{\|\nabla I_{\text{BIAS}}(k)\|} = \frac{\nabla M(k)}{\|\nabla M(k)\|}, \quad (10)$$

demonstrating the invariance of normalised gradient-based similarities with respect to  $B$ . Nevertheless, as suggested by our results, squaring the dot product as in [10], accentuates the contribution of the normalisation factors  $\varrho$  and  $\tau$ , yielding a slightly lower performance.

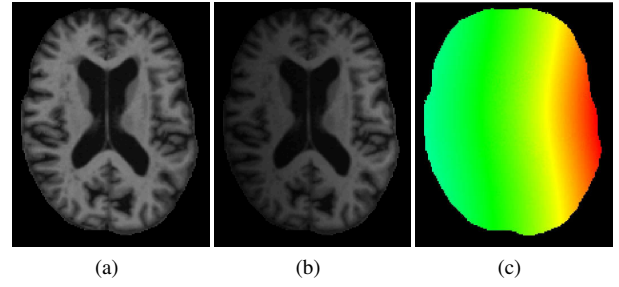


**Fig. 1.** Axial view of one of the T1-weighted brain images utilised. (a): Original. (b): With simulated bias field. (c): Rainbow-coded bias field

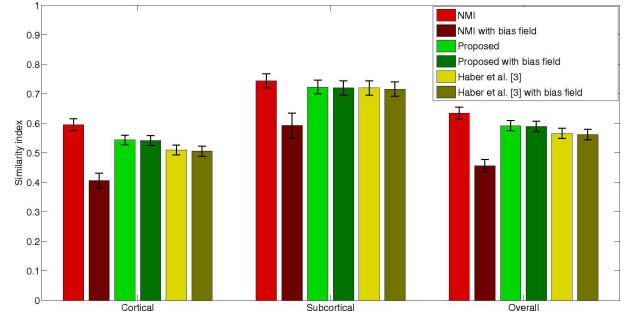


**Fig. 2.** Mean similarity index and standard deviation over cortical and subcortical labels for all  $34 \times 33 = 1122$  registrations.

#### 2.3.2. Robustness against general mismatches

As we later show in our results, the similarity measure presented in [10], is not robust against general mismatches. This is because  $\cos^2 \phi$  has strictly positive values. Therefore, in the region of mismatches  $\Omega_0$  we have  $\sum_{k \in \Omega_0} \cos^2 \phi(\nabla I_0(k), T(\nabla I(k))) \gg 0$ . Consequently, the total cost function can be arbitrarily biased by the presence of outliers. In contrast, the histogram of the inner product of the normalised gradients taken from  $\Omega_0$  has a distribution of zero mean. Hence,  $\sum_{k \in \Omega_0} \cos \phi(\nabla I_0(k), T(\nabla I(k))) \approx 0$ , which means that the presence of outliers do not bias the proposed similarity measure.

## 3. RESULTS

As previously mentioned, we incorporate the proposed measure into a B-Spline FFD approach [15]. For comparison, we also incorporate the cosine squared similarity [10] and normalised mutual information (NMI) [9] into our framework. In all the conducted experiments, we utilise the bending energy of the deformation field as regularisation term  $E_R$  and we set the noise filtering parameter  $\eta$  to 0.01. We also set  $\lambda = 0.01$  for registrations optimising NMI and  $\lambda = 0.0001$  for registrations optimising gradient-based similarities. We further regularise the forces for the gradient-based methods using a gaussian kernel with  $\sigma$  equal to 4 times the (isotropic) voxel size.

### 3.1. MR images with intensity inhomogeneities

Here, we evaluate the performance of our similarity against intensity inhomogeneities. This relaxes the necessity of an explicit intensity correction step in the registration pipeline, which can be time

**Table 1. Images with pathology:** Overlap measures for white matter (WM), gray matter (GM) and cerebrospinal fluid (CSF) labels propagated using the proposed similarity and Haber *et al.* [10]. Bold means statistically significant with  $p = 0.001$

	WM	GM	CSF	Overall
Proposed similarity	<b>79.2</b>	<b>78.3</b>	<b>62.0</b>	<b>73.2</b>
Haber <i>et al.</i> [10]	77.0	77.2	61.0	71.7

consuming and a potential source of errors, especially for non-brain images.

For this experiment, we employ 34 T1-weighted MR brain images, which have been manually segmented by experts<sup>1</sup> into 134 anatomical structures. We perform the  $34 \times 33 = 1122$  pairwise registrations with control point spacings of 20, 10, 5 and 2.5mm, using the original images. We subsequently introduce different smooth intensity inhomogeneities individually to all the images using a MATLAB tool<sup>2</sup> and perform the same registrations again using the original images as target and the affected ones as source. Figure 1 shows an example image with and without bias field.

We compare the gradient-based similarity measures against NMI in their ability to produce a deformation field able to accurately propagate the manual segmentation labels. We measure the registration accuracy using the similarity index (SI), both for the original images and the images with bias field. We compute the mean and standard deviation of the SI values calculated on the propagated and reference labels for all 1122 propagations. We differentiate between 98 cortical and 36 subcortical labels. We observe that NMI performs good when there is no intensity inhomogeneities in the images. On the contrary, it is severely affected by the presence of intensity inhomogeneities. Conversely, both gradient-based similarities show similar performances for registrations with and without intensity inhomogeneities, demonstrating their robustness. Nevertheless, the proposed similarity performs better than cosine squared. As we mention in section 2.3.1, this difference in performance might be caused by the increased influence of the normalisation factors when squaring the dot product. Detailed results are shown in Figure 2.

It is important to note that in the case where no intensity inhomogeneities are present, the proposed method has a lower performance than NMI. The conducted analyses suggest that, when using normalised gradient fields, the registration of MR images is more difficult than the alignment of scans from other imaging modalities as in [11, 12, 13]. We observe that in the particular case of MR brain images, the discrimination between noise- and structure-related gradients is very challenging, especially in cortical areas. This also renders the choice of the noise parameter  $\eta$  more difficult and demands an aggressive regularisation of the force field.

### 3.2. MR images with pathologies

Registration of images depicting pathology is a challenging procedure, since the images may exhibit strong structural differences that cannot be matched. Here, we show that our similarity measure is capable of handling images with areas of mismatches, e.g., areas of pathology, without any prior knowledge nor any subsequent correction step.

For this experiment, we take 10 brain images with simulated tumours from the BraTS MICCAI challenge image database. Half

<sup>1</sup>provided by Neuromorphometrics, Inc. under academic subscription. ([www.neuromorphometrics.com](http://www.neuromorphometrics.com))

<sup>2</sup>[bigwww.epfl.ch/algorithms/mri-reconstruction](http://bigwww.epfl.ch/algorithms/mri-reconstruction)

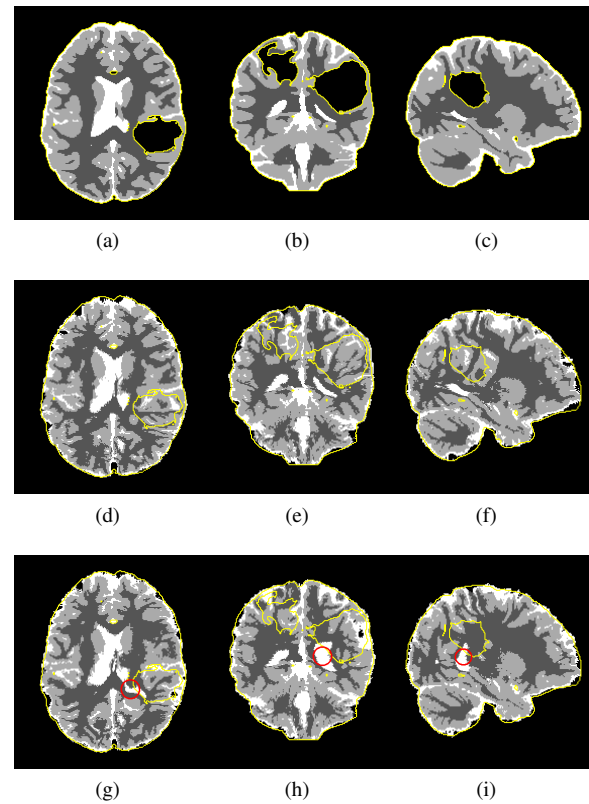


**Fig. 3.** Reference and propagated labels. (a)-(c): Reference. (d)-(f): Propagated using proposed similarity. (g)-(i): Propagated using Haber *et al.* [10]. Boundaries of the tumours and image are provided for visualisation.

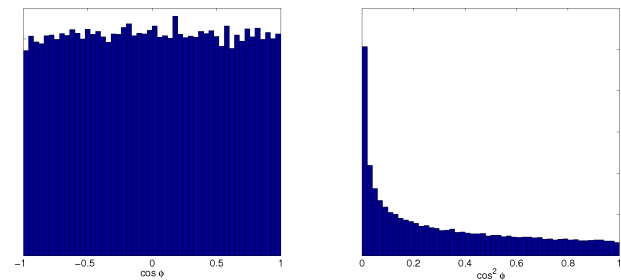


**Fig. 4.** Histograms of  $\cos \phi$  and  $\cos^2 \phi$  between a healthy subject and the BraTS simulated images in the tumour areas. The means are 0.002 and 0.330, respectively.

of these images show high grade gliomas and the other half has low grade ones. These images are labelled into white matter (WM), gray matter (GM), cerebrospinal fluid (CSF) and 2 further labels for the tumour areas. For a quantitative evaluation, a labelled image of a healthy subject that was used to simulate the tumours is registered to the 10 BraTS images. We measure the registration accuracy using SI over the three labels WM, GM and CSF. We ignore the two available tumour labels as there is no equivalent in the healthy scan. A good overlap for non-tumour labels means that the similarity measure is not biased by the presence of pathology. Table 1 shows the overlaps obtained by the proposed method compared to cosine

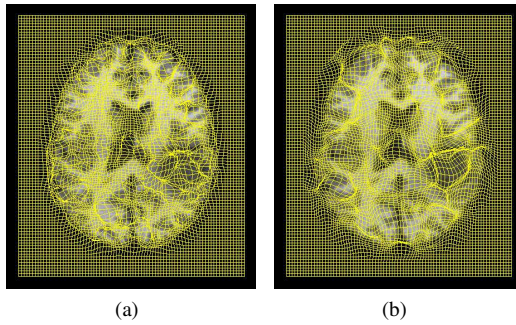


**Fig. 5.** Axial view of deformation fields produced by (a) NMI (1.26% of voxels with negative jacobian) and (b) proposed method (0.13% of voxels with negative jacobian).

squared. We observe better overall alignment, thus demonstrating increased robustness against the presence of tumours. Visual results are shown in Figure 3. The main areas where the registration is affected by the tumour presence are highlighted by a red circle. This effect is further supported by the experimental evidence that for the tumour areas, the histogram of the cosine values has a distribution with zero mean, as shown in Figure 4. Hence, the sum of these values has an expected value of zero. On the contrary, the histogram for cosine squared demonstrates that the distribution of its values in the tumour areas has a strictly positive value, thus biasing the energy computation.

Another interesting fact is that with the proposed similarity measure and regularisation, a smoother (hence, more plausible) deformation in the tumour area than with NMI is obtained, as shown in Figure 5.

#### 4. CONCLUSION

In this work, we have proposed a similarity measure for medical image registration that is robust towards bias fields and outliers in form of pathologies. We demonstrate the effectiveness and robustness of our similarity measure on images with simulated bias fields and on simulated pathological images, showing superior robustness in these scenarios compared to NMI and the cosine squared measure of Haber *et al.* [10].

The main contribution of this paper is that our similarity measure, relaxes the need of using preprocessing steps like bias field correction, which can be time consuming and prone to errors. Also, it can be utilised to register images in the presence of pathologies, since it does not rely on any particular deformation model and does not require segmentations of the outliers.

As future work, we plan to investigate possible extensions to the proposed method, in order to be able to deal with multimodal registrations tasks such as T1-T2 MRI registration.

## Acknowledgment

This work was partially funded by CONICYT.

#### 5. REFERENCES

[1] A. Sotiras, C. Davatzikos, and N. Paragios, “Deformable medical image registration: a survey,” *IEEE transactions on med-*

*ical imaging*, vol. 32, no. 7, pp. 1153–90, July 2013.

[2] F.J.P. Richard, “A new approach for the registration of images with inconsistent differences,” in *International Conference on Pattern Recognition (ICPR)*, 2004, vol. 5, pp. 5–8.

[3] E.I. Zacharaki, D. Shen, S. Lee, and C. Davatzikos, “ORBIT: a multiresolution framework for deformable registration of brain tumor images,” *IEEE transactions on medical imaging*, vol. 27, no. 8, pp. 1003–17, Aug. 2008.

[4] M. Hachama, A. Desolneux, and F.J.P. Richard, “Bayesian Technique for Image Classifying Registration,” *IEEE Transactions on image processing*, vol. 21, no. 9, pp. 4080–4091, 2012.

[5] C. Studholme, C. Drapaca, B. Iordanova, and V. Cardenas, “Deformation-based mapping of volume change from serial brain MRI in the presence of local tissue contrast change,” *IEEE transactions on medical imaging*, vol. 25, no. 5, pp. 626–39, May 2006.

[6] D. Loeckx, P. Slagmolen, F. Maes, D. Vandermeulen, and P. Suetens, “Nonrigid image registration using conditional mutual information,” *IEEE transactions on medical imaging*, vol. 29, no. 1, pp. 19–29, 2010.

[7] X. Zhuang, S. Arridge, D.J. Hawkes, and S. Ourselin, “A non-rigid registration framework using spatially encoded mutual information and free-form deformations,” *IEEE transactions on medical imaging*, no. c, pp. 1–10, 2011.

[8] J.P.W. Pluim, J.B. Maintz, and M. Viergever, “Image registration by maximization of combined mutual information and gradient information,” *IEEE transactions on medical imaging*, vol. 19, no. 8, pp. 809–14, Aug. 2000.

[9] C. Studholme, D.L.G. Hill, and D.J. Hawkes, “An overlap invariant entropy measure of 3D medical image alignment,” *Pattern Recognition*, vol. 32, no. 1, pp. 71–86, Jan. 1999.

[10] E. Haber and J. Modersitzki, “Intensity gradient based registration and fusion of multi-modal images,” in *Medical image computing and computer-assisted intervention : MICCAI*, Jan. 2006, vol. 46, pp. 292–9.

[11] S. Heldmann and S. Zidowitz, “Elastic registration of multi-phase CT images of liver,” in *Proc. of SPIE*, David R. Haynor and Sébastien Ourselin, Eds., 2009.

[12] T. Lange, N. Papenberg, S. Heldmann, J. Modersitzki, B. Fischer, H. Lamecker, and P.M. Schlag, “3D ultrasound-CT registration of the liver using combined landmark-intensity information,” *International journal of computer assisted radiology and surgery*, vol. 4, no. 1, pp. 79–88, Jan. 2009.

[13] J. Rühaak, L. König, M. Hallmann, N. Papenberg, S. Heldmann, H. Schumacher, and B. Fischer, “A Fully Parallel Algorithm For Multimodal Image Registration Using Normalized Gradient Fields,” in *International Symposium on Biomedical Imaging (ISBI)*, 2013, pp. 572–575.

[14] G. Tzimiropoulos, S. Zafeiriou, and M. Pantic, “Robust and efficient parametric face alignment,” in *International Conference of Computer Vision (ICCV)*, 2011.

[15] D. Rueckert, L.I. Sonoda, C. Hayes, D.L.G. Hill, M.O. Leach, and D.J. Hawkes, “Nonrigid registration using free-form deformations: application to breast MR images,” *IEEE transactions on medical imaging*, vol. 18, no. 8, pp. 712–21, Aug. 1999.